

Spin Glass Behavior in the Frustrated Antiferromagnetic LiNiO_2

JAN N. REIMERS AND J. R. DAHN

Department of Physics, Simon Fraser University, Burnaby, British Columbia, Canada, V5A 1S6

J. E. GREEDAN, C. V. STAGER, AND G. LIU

Institute for Materials Research, McMaster University, 1280 Main Street West, Hamilton, Ontario, Canada, L8S 4M1

I. DAVIDSON

Institute for Environmental Chemistry, National Research Council of Canada, Montréal Road, Ottawa, Ontario, Canada, K1A 0R6

AND U. VON SACKEN

Moli Energy (1990) Limited, 3958 Myrtle Street, Burnaby, British Columbia, Canada, V5C 4G2

Received June 2, 1992; in revised form July 20, 1992; accepted July 21, 1992

LiNiO_2 is a member of the solid solution series $\text{Li}_x\text{Ni}_{2-x}\text{O}_2$ and has been suggested as an experimental spin $\frac{1}{2}$ triangular lattice antiferromagnet. It is therefore thought to be a good candidate for spin liquid behavior. We have carried out detailed structural studies using powder X-ray and neutron diffraction with Rietveld profile refinement on five different samples of $\text{Li}_x\text{Ni}_{2-x}\text{O}_2$ with x near 1. The results show that there are always some nickel atoms occupying sites in the lithium layers even when $x = 1$. We show that the presence of nickel atoms in these sites profoundly affects the magnetic behavior and can easily explain the differences in magnetic behavior for LiNiO_2 previously reported in the literature. Magnetic susceptibility data on these samples show high temperature behavior similar to previously reported results. At low temperatures spin glass freezing is observed at $T_f = 9$ K for samples with $x \approx 1$. Low-field measurements on such samples are necessary in order to see this clearly. A simple exchange model is proposed which explains most of the experimental results, thus showing that the spin liquid interpretation of previous workers is unnecessary. © 1993 Academic Press, Inc.

Introduction

Since Anderson first proposed his resonating valence bond (RVB) theory of high-temperature superconductivity (1) there has been considerable interest in frustrated spin

systems which show potential for RVB or spin liquid ground states. The $S = \frac{1}{2}$ Heisenberg triangular lattice antiferromagnet was the first system for which an RVB ground state was considered likely (2). Since then a host of other lattices (square (3), Kagome

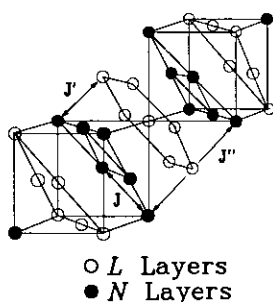


FIG. 1. Schematic representation of the metal atom layers in $\text{Li}_x\text{Ni}_{2-x}\text{O}_2$. The *L* layers are predominantly lithium and the *N* layers are predominantly nickel. The in-plane (*J*) and two interplane (*J'* and *J''*) magnetic exchange constants are also shown.

(4), and the corner sharing tetrahedra (5) lattices) have shown promise for RVB behavior. Perhaps the most famous of these is the 2-d square lattice formed by Cu^{2+} atoms in $\text{YBa}_2\text{Cu}_3\text{O}_{6+\delta}$.

Hirakawa has suggested that LiNiO_2 is a good candidate for spin liquid behaviour (6). A spin liquid has no Néel-like sublattice order and cannot be described in terms of spin wave theory. It is not easy to prove the presence of the spin liquid phase experimentally since there will be no magnetic Bragg scattering. It is not known whether or not short range correlations in the RVB ground state will be strong enough to show diffuse magnetic scattering. Finite temperature behavior of RVB models is also poorly understood. In this work we will show that there is almost always some degree of disorder in LiNiO_2 and that the magnetic properties are consistent with that of a spin glass. The RVB model is therefore deemed unnecessary or inappropriate for this material.

The LiNiO_2 structure is based on layers of close packed oxygen atoms, and the metal atoms form a face-centered cubic array with a weak trigonal distortion. Perpendicular to the distortion are alternating (111) planes of metal atoms which we label *L* and *N* in Fig. 1. Near $x = 1$ in $\text{Li}_x\text{Ni}_{2-x}\text{O}_2$ the *L* planes

are predominantly occupied by lithium atoms and the *N* planes are mostly nickel. Because of the pseudo *fcc* packing of the metal atoms the *L* and *N* planes form triangular networks that stack with the ($\dots\text{LNLNLN}\dots = \dots\text{ABCABC}\dots$) rhombohedral stacking. Hence metal atoms in neighboring layers are situated above and below the centers of the in-plane triangles. Magnetic properties will be dominated by the *N* planes which are also stacked in the rhombohedral sense. Because of this some authors have claimed that interplane interactions will cancel by symmetry resulting in strictly 2-d magnetism. However, this is not correct and interplane interactions will have a profound effect on both the in-plane correlations and also on the bulk magnetic properties (7). Most previous magnetic studies of this material ignored the fact that LiNiO_2 should be considered as a member of the series $\text{Li}_x\text{Ni}_{2-x}\text{O}_2$ ($0 \leq x \leq 1$) (8, 9). When $x < 1$, Ni occupies positions in *L* layers which immediately implies disorder in any spin model describing the system.

Goodenough (8) first studied LiNiO_2 as part of the series $\text{Li}_x\text{Ni}_{2-x}\text{O}_2$ and reported ferrimagnetism for $0.6 < x < 1.0$, and a Weiss constant θ that increased as x decreased from 1.0. More recent experimental work on the magnetic properties of LiNiO_2 has lead to claims of spin liquid behavior (6), ferrimagnetism (6), ferromagnetism (10), and a *new* type of frozen spin state (11). Neutron diffraction experiments show no conclusive signs of diffuse scattering near the $(\frac{1}{3}, \frac{1}{3}, l)$ Bragg angles, even at 1.4 K (6, 12). Small angle neutron scattering experiments show a steady increase in the scattering at low *Q* (scattering vector), interpreted as an onset of ferromagnetic correlations below $T \approx 240$ K. Bulk susceptibility measurements on LiNiO_2 have led to a good deal of confusion. In most reports Curie-Weiss law behavior is observed above $T \approx 240$ K, yielding Ni^{3+} moments consistent with $S = \frac{1}{2}$ (assuming $g = 2$) and Weiss

constants, θ , ranging from $-65(20)$ K (6) to $79(5)$ K (11). Below $T \approx 240$ K the deviation from Curie–Weiss behavior is indicative of ferromagnetic correlations. Nonlinearities in M vs H are observed below 240 K and at 4.2 K no saturation in M is observed, suggesting antiferromagnetic correlations. Hysteresis is observed below $T \approx 20$ K (6). Heat capacity measurements (11) reveal complete magnetic entropy removal between 300 and 0.4 K with no noticeable anomalies that could be associated with a transition to long-range order. Kemp, Cox, and Hodby (10) have stated that many of the above results are consistent with a 2-d Ising ferromagnet with $T_c \approx 6$ K. They support their claims with a determination of the critical exponent γ . However, the temperature range investigated seems to be outside of the supposed critical regime.

LiNiO_2 has been proposed as an electrode material in secondary Li batteries because Li can be electrochemically de-intercalated to form $\text{Li}_{1-y}\text{NiO}_2$. The capacity of the batteries (the amount of Li that can be reversibly removed) is found to be highly correlated with the stoichiometry of the starting material (x in $\text{Li}_x\text{Ni}_{2-x}\text{O}_2$). Therefore a great deal of work has been carried out by the battery makers regarding the synthesis of LiNiO_2 (18). For battery applications, samples with as little Ni in the L layers as possible and those with x as close to 1 as possible are desirable.

Here we investigate the magnetic properties of five $\text{Li}_x\text{Ni}_{2-x}\text{O}_2$ samples with x near 1, prepared under different conditions. We have made detailed structural studies of the samples using powder X-ray and neutron diffraction with Rietveld profile refinement. We show the dependence of the magnetic properties on sample stoichiometry. For the two most crystallographically ordered samples, a downturn in the zero field cooled susceptibility at 9 K is observed, indicating the onset of strong antiferromagnetic correlations below this temperature. This has not

been previously observed. Finally, an attempt is made to understand the magnetic properties in terms of a suitable exchange model.

Experimental

Two samples labeled A and B were prepared at Moli Energy (1990) Limited, Burnaby, British Columbia, Canada. $\text{LiOH} \cdot \text{H}_2\text{O}$ and NiO were ground in a 1.1 : 1 Li : Ni ratio which hinders Ni occupation in the layers. The mixture was heated for $4\frac{1}{2}$ hr at 650°C , ground and reheated for another $12\frac{1}{2}$ hr at 650°C , all in moisture-free and CO_2 -free air. A third firing at 650°C for 4 hr was carried out at two different humidities corresponding to dew points of 0°C for A and -40°C for B. The other three samples (labeled C, D, and E) were prepared at the National Research Council (NRC) from equal weight mixtures of Anachemia reagent grade $\text{LiOH} \cdot \text{H}_2\text{O}$ and Aldrich nickel peroxide hydrate. The equal weight mixture again ensures excess Li in the starting mixture. The mixtures were ground, pelletized, and loaded into gold crucibles. Two samples were heated under O_2 for 3 hr at 200°C , followed by 52 hr (C) and 35 hr (D) at 800°C . E was also heated under O_2 but for 2 hr at 200°C , followed by 40 hr at 650°C . All products were washed with water, then ethanol, and were finally dried for several hours at 110°C . Two of the three NRC samples D and E were heated to a temperature similar to that of samples used in previous magnetic studies (6, 10, 11), notably higher than the heating temperature of samples A and B. Hirota *et al.* have found that prolonged heating at 800°C results in a progressive loss of lithium from LiNiO_2 and substitution of Ni for Li (11).

X-ray diffraction measurements were made using a Phillips powder diffractometer with a diffracted beam monochromator and a copper target X-ray tube. Neutron diffraction data were collected at the McMaster

Nuclear Reactor using 1.3913 Å neutrons and a position sensitive detector (13) that simultaneously collects useful data over a range of 25° in 2θ. Rietveld refinements were carried out using the Hill and Howard (14) package which was modified locally by H. D. Grundy for the McMaster detector geometry. All X-ray and neutron diffraction data were collected at room temperature.

Magnetic susceptibility data were collected on a Quantum Design SQUID magnetometer using pressed pellets. The SQUID was calibrated with high purity palladium.

Crystal Structure

All structural refinements were carried out in the space group $R\bar{3}m$ with Ni, Li, and O at Wyckoff positions 3a, 3b, and 6c, respectively. To allow for disorder, the parameter x in Li_{*x*}Ni_{2-*x*}O₂ was refined and a fraction δ of the sites in the *L* planes were allowed to be occupied by Ni. Thus we have the four occupations,

$$\begin{array}{l}
 L \text{ planes} \left\{ \begin{array}{l} \text{fraction of sites occupied by Li;} \\ L(\text{Li}) = 1 - \delta \\ \text{fraction of sites occupied by Ni;} \\ L(\text{Ni}) = \delta \end{array} \right. \\
 \\
 N \text{ planes} \left\{ \begin{array}{l} \text{fraction of sites occupied by Li;} \\ N(\text{Li}) = x - 1 + \delta \\ \text{fraction of sites occupied by Ni;} \\ N(\text{Ni}) = 2 - x - \delta, \end{array} \right.
 \end{array}$$

which satisfy the constraints

$$\begin{aligned}
 N(\text{Li}) + L(\text{Li}) &= x, \\
 N(\text{Ni}) + L(\text{Ni}) &= 2 - x \quad (1a)
 \end{aligned}$$

$$\begin{aligned}
 N(\text{Li}) + N(\text{Ni}) &= 1, \\
 L(\text{Li}) + L(\text{Ni}) &= 1. \quad (1b)
 \end{aligned}$$

Individual temperature factors on Ni and O were found to be highly correlated with x and δ . Therefore our refinements included only an overall temperature factor which was not highly correlated with x and δ , resulting in more reliable values for these parameters. Results for all five samples from

the X-ray Rietveld refinement are shown in Table I. Only the A and B samples were large enough for neutron diffraction and the Rietveld results for these are in Table II. Figure 2 shows the profile fits for A; the profiles for B were very similar. The results show that x is closer to 1 and δ is smaller for samples A and B. The unit cell constants are smaller for A and B, consistent with the largest lithium concentrations because larger cell constants are a sign of Li deficiency (8, 15). Cell constants were also obtained from least-squares refinement of the X-ray peak positions which included a correction for off-axis displacement (16) of the sample in the goniometer. These results are shown in Table III and are consistent with the Rietveld results.

A further sensitive test of the stoichiometry is the ratio of the X-ray Bragg intensities

$$R = \frac{I(006) + I(10\bar{2})}{I(101)}. \quad (2)$$

For $x = 1$ and $\delta = 0$, $R = 0.411$. As x in Li_{*x*}Ni_{2-*x*}O₂ increases, R rapidly does the same. Figure 3 shows R vs x calculated, assuming $\delta = 1 - x$, by PULVERVIX (17), which was used to extract x values from measured R values. An analytic approximation (18)

$$R = \frac{4}{3} \left(\frac{1.6 - x}{x} \right)^2, \quad (3)$$

which does not take into account the differences in the dependence of the nickel and oxygen atomic form factors with scattering angle, is also included in Fig. 3. The intensities $I(hkl)$ were determined in two ways: (1) by numerically integrating the data after background subtraction and (2) from a least-squares fit to the data with a Gaussian peak shape. The first method is believed most accurate as the real peak shapes are only approximately Gaussian. The results are shown in Table IV which again indicate that samples A and B are the closest to being

TABLE I

CRYSTALLOGRAPHIC PARAMETERS FOR $\text{Li}_x\text{Ni}_{1-x}\text{O}_2$ OBTAINED FROM RIETVELD REFINEMENT OF X-RAY DATA

Sample	a (Å)	c (Å)	z	B (Å ²)	x	δ	R_{wp}	R_{exp}	R_{Br}
A	2.8769(1)	14.198(1)	0.2580(3)	0.49(5)	1.01(1)	0.022(3)	11.7	9.0	2.32
B	2.8764(1)	14.195(1)	0.2576(3)	0.42(6)	1.02(1)	0.015(3)	12.4	9.0	2.41
C	2.8833(1)	14.217(2)	0.2611(4)	0.88(8)	0.96(1)	0.048(4)	14.5	9.0	2.79
D	2.8813(1)	14.209(1)	0.2580(3)	0.57(6)	0.97(1)	0.032(3)	12.9	8.8	2.50
E	2.8848(1)	14.233(2)	0.2574(4)	0.70(8)	0.90(1)	0.108(4)	12.8	8.6	2.67

Note. z is the oxygen fractional coordinate, B is the overall temperature factor, and δ is the occupation of Ni in the L planes (see text). $R_{\text{wp}}^2 = [\sum w(y_{\text{obs}} - y_{\text{calc}})^2] / [\sum w y_{\text{obs}}^2]$ and $R_{\text{exp}}^2 = [N - P] / [\sum w y_{\text{obs}}^2]$, where the summations are over all data points, y_{obs} and y_{calc} are observed and calculated intensities, $w = 1/y_{\text{obs}}$ is the corresponding weight, N is the number of data points, and P is the number of refined parameters. $R_{\text{Br}} = [\sum |I_{\text{obs}} - I_{\text{calc}}|] / [\sum I_{\text{obs}}]$, where the summations are over all reflections, and I_{obs} and I_{calc} are the observed and calculated intensities of each reflection.

stoichiometric. The integrated intensity method is useful for three reasons: (1) it is simple and accurate, (2) it avoids problems due to parameter correlations in the Rietveld method, and (3) previously published peak intensities can be compared to estimated sample stoichiometry for literature materials. In particular, Hirota's (11) published X-ray intensity for the 101 peak (no 006 or 10 $\bar{2}$ intensities were reported) is only 81% of the expected value, indicating that $x \approx 0.7$.

We have clearly shown that these samples (and those in the literature) have some degree of cation mixing; nickel in L layers and lithium in N layers, even if $x = 1$. When $x < 1$, the cation mixing becomes larger. The two samples A and B are the most stoichiometric and have the least mixing of cat-

ions. Based on the integrated intensities A appears to be very close to stoichiometric. B seems to be nickel deficient but this may be misleading due to the weak dependence of R on x for $x > 1$. As we shall see the stoichiometry has a profound effect on the low-temperature magnetic properties.

Magnetism

Here we focus on measurements that have not previously been attempted on LiNiO_2 , to our knowledge. These are: (1) low field ($H < 0.1$ T) susceptibility, (2) measurement at 0.001 T after cooling in zero field and after cooling in 0.05 T, and (3) relaxation of the magnetization with time after the field was changed from 0.05 T to 0.001 T. First, however, we present the Curie-Weiss

TABLE II

CRYSTALLOGRAPHIC PARAMETERS FOR $\text{Li}_x\text{Ni}_{1-x}\text{O}_2$ OBTAINED FROM RIETVELD REFINEMENT OF THE NEUTRON DATA

Sample	a (Å)	c (Å)	z	B (Å ²)	x	δ	R_{wp}	R_{exp}	R_{Br}
A	2.8729(1)	14.174(1)	0.2592(1)	0.28(2)	0.98(1)	0.028(3)	4.9	2.5	1.65
B	2.8731(1)	14.180(1)	0.2587(1)	0.40(6)	0.97(1)	0.026(3)	5.7	3.0	1.40

Note. z is the oxygen fractional coordinate, B is the overall temperature factor, and δ is the occupation of Ni in the L planes (see text). R_{wp} , R_{exp} , and R_{Br} are defined in the caption for Table I.

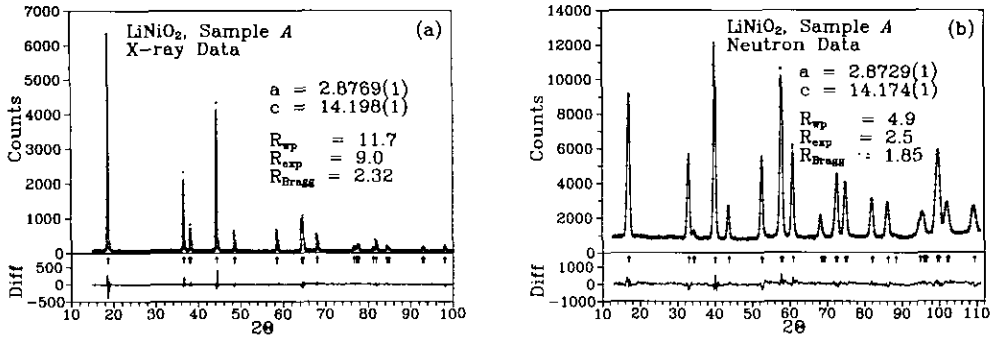


FIG. 2. (a) Observed (+), calculated (-), and difference (bottom) X-ray diffraction profiles for the LiNiO_2 sample A. Bragg reflection positions are marked by arrows (\uparrow). (b) As in part (a) for the neutron data.

(CW) law fits (Fig. 4) to the high-temperature data for two of our samples A and B. All data were corrected for diamagnetism. The fits were made on data in the range $220 \text{ K} \leq T \leq 300 \text{ K}$, giving $\theta = 26(10) \text{ K}$, $\mu = 2.1(1) \mu_B$, and $\theta = 2(10) \text{ K}$, $\mu = 2.2(1) \mu_B$ for A and B, respectively. The θ s are intermediate to previously reported values, $\theta = -65(20) \text{ K}$ (6), $\theta = 60(?) \text{ K}$ (10), and $\theta = 79(5) \text{ K}$ (11). The moments are slightly higher than the spin-only value $\mu_{s.o.} = 1.73 \mu_B$, and assuming $g = 2$ the measured moments correspond to $S = 0.66(2)$ and $S = 0.71(2)$, respectively. These values of S should be compared with the literature values, $S = 0.55$ (6), 0.85 (11), and 0.95 (10).

We believe all of these results are suspect including our own. None of the other work-

ers have attempted to correct their data for diamagnetism, which will be important at high temperatures where χ is small. Data above 300 K are vital for a proper determination of μ and especially θ . Kemp *et al.* fit data in the range $100 \text{ K} \leq T \leq 250 \text{ K}$ with only two data points above 200 K , thus almost all of their data is outside the linear regime. The data of Hirota *et al.* extend up to 400 K but their data quality at these temperatures seem to be poor. Hirakawa *et al.* have measured six data points between 400

TABLE III
CELL CONSTANTS AND CELL VOLUMES FOR THE HEXAGONAL CELL OBTAINED FROM LEAST-SQUARES FITTING OF THE PEAK POSITIONS

Sample	a (\AA)	c (\AA)	Vol. (\AA^3)	χ^2
A	2.8765(2)	14.188(2)	101.67(3)	0.071
B	2.8766(2)	14.182(2)	101.63(3)	0.063
C	2.8814(5)	14.193(5)	102.18(3)	0.126
D	2.8811(3)	14.196(3)	102.05(3)	0.092
E	2.8822(6)	14.207(8)	102.21(9)	0.187

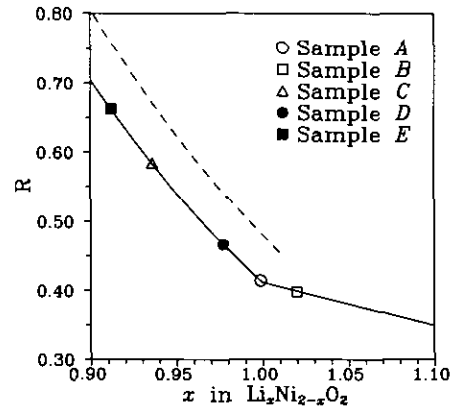


FIG. 3. Peak intensity ratio $R = \{I(006) + I(102)\}/I(101)$, calculated using PULVERIX (17) for $\delta = 1 - x$, as a function of x in $\text{Li}_x\text{Ni}_{2-x}\text{O}_2$. The analytic approximation, Eq. (3), is shown by a dashed line.

TABLE IV
 x IN $\text{Li}_x\text{Ni}_{2-x}\text{O}_2$ OBTAINED FROM THE PEAK
 INTENSITY RATIO $R = \{I(006) + I(10\bar{2})\}/I(101)$

Sample	R_{int}	x_{int}	R_{fit}	x_{fit}
A	0.414(7)	0.999(3)	0.425(13)	0.994(6)
B	0.398(7)	1.02(1)	0.411(19)	1.00(3)
C	0.584(11)	0.936(3)	0.608(23)	0.935(5)
D	0.467(8)	0.977(3)	0.473(12)	0.975(4)
E	0.663(12)	0.912(3)	0.707(23)	0.919(3)

R was determined in two ways: (1) from numerical integration after background subtraction and (2) from a least-squares fit to the data with a Gaussian peak shape. $R = 0.411$ corresponds to $x = 1.0$.

and 600 K which appear linear in χ^{-1} vs T , and one can see from their data that fitting to data below 400 K results in a larger slope and therefore a larger moment as well as an overestimate of θ . Hirakawa's fit understandably resulted in the lower moment and the lowest θ . The most one can conclude from this is that strong ferromagnetic interactions must be present to explain the high-temperature deviations from CW behavior in all samples studied to date. From our data it is evident that below $T \approx 50$ K this trend toward ferromagnetic correlations starts to reverse itself.

Figure 5 shows the history dependence of the magnetism at low temperatures for all five samples. For these measurements the sample was first zero-field cooled (*zfc*) to 4 K, and measured at $H = 0.001$ T while warming to 80 K. Then the sample was field cooled (*fc*) at $H = 0.05$ T and remeasured at $H = 0.001$ T while warming. Figure 5a shows weak history dependence between 9 K and 60 K and dramatic irreversibilities below 9 K for samples A and B. The susceptibility maximum or cusp at 9 K for the *zfc* samples has not been observed previously. The data for samples A and B are fully consistent with spin glass freezing at $T_f \approx 9$ K. The results for the three samples C, D, and E shown in Fig. 5b are markedly different.

The history dependence is much stronger in the temperature range $9 \text{ K} \leq T \leq 60 \text{ K}$ and the *fc* magnetization is also much larger. Although not obvious on the scale used, two of the samples, C and D, both have maxima near 9 K as is the case in Fig. 5a. Clearly the ferromagnetic interactions in these three samples are much stronger.

For all samples, field cooling ($H = 0.05$ T) to 5 K and then removing the applied field resulted in relaxation of the magnetization over macroscopic time scales. A sample data set for B is shown in Fig. 6. The solid line represents a fit to the empirical relationship

$$M(T) = M_1 e^{-t/\tau_1} + M_2 e^{-t/\tau_2}, \quad (4)$$

where τ_1 and τ_2 are relaxation times. Attempts to model the data with only one relaxation time resulted in a decidedly poor fit to the data. We do not attach much importance to the quantitative results of this analysis except to say that the relaxation probably occurs on many time scales (most of which are outside the resolution of this experiment), which is again consistent with spin glass behavior (19) where one expects to see a distribution of relaxation times. Similar effects were observed in the other samples.

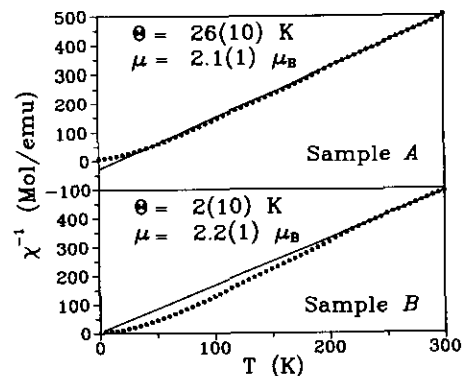


FIG. 4. Fit of the high-temperature ($220 \text{ K} \leq T \leq 300 \text{ K}$) susceptibility to a Curie-Weiss law $\chi^{-1} = (T - \theta)/C$ for two samples, A and B.

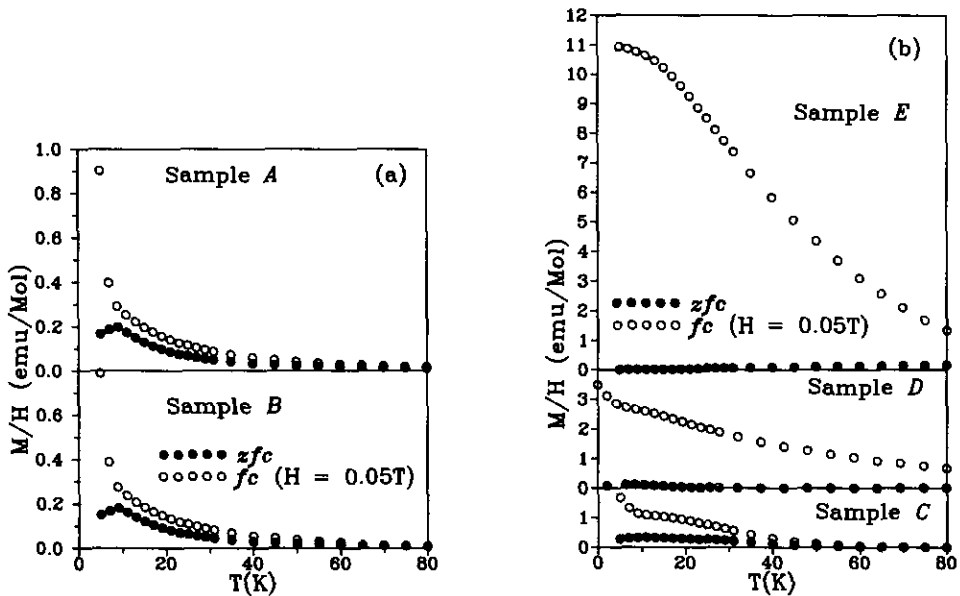


FIG. 5. (a) Field cooled (\circ , $H = 0.05$ T) and zero field cooled (\bullet , $H =$ residual) susceptibilities measured at $H = 0.001$ T for two samples, A and B, showing spin glass freezing at $T_f = 9$ K. (b) As in part (a) for the three remaining samples C, D, and E, showing much stronger irreversibilities over a wider temperature range.

Discussion and Conclusions

We have shown the intimate relationship between bulk magnetic properties of $\text{Li}_x\text{Ni}_{2-x}\text{O}_2$ and sample stoichiometry. Five samples with different stoichiometries have been investigated with X-ray and neutron diffraction. We showed that x in $\text{Li}_x\text{Ni}_{2-x}\text{O}_2$ varied from 0.90(1) to 1.02(1) depending on the sample preparation and the method of determining x . Samples A and B were closest to being stoichiometric and had the least amount of nickel in the L layers. These two samples showed spin glass behavior in the form of strong irreversibilities below the freezing temperature $T_f = 9$ K, a cusp in the zfc susceptibility, and relaxation over multiple time scales below T_f . The other samples C, D, and E showed irreversibilities over a wider temperature range and much larger magnetizations than for fc samples.

A qualitative understanding of these re-

sults can be obtained without resorting to exotic ideas of spin liquid behavior. Clearly there must be both ferromagnetic and antiferromagnetic exchange interactions in this material. Here we propose a simple exchange model which explains most of the experimental results. We retain the standard in-plane antiferromagnetic interaction $J < 0$, which results in frustration on the triangular network of spins in the N layers. In the absence of strong anisotropy the classical ground state will be a non-collinear spin arrangement with neighboring spins oriented at 120° angles to each other (20). A ferromagnetic interaction $J' > 0$ couples nickel atoms in the L layers to spins in the N planes above and below, which are predominantly nickel. As the basal plane bond lengths are roughly the same as the metal-metal distances between the L and N layers, it is quite possible that J' is stronger than J . Goodenough has pointed out (8) that the

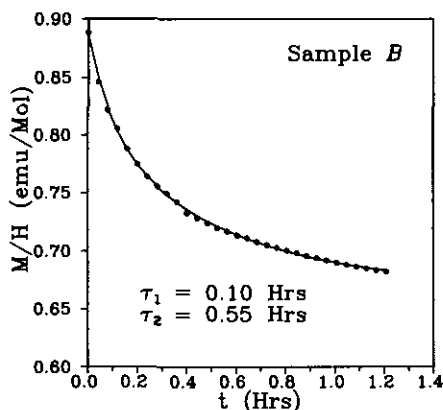


FIG. 6. An example of the relaxation phenomena at $T = 5$ K, observed in field ($H = 0.5$ T) cooled samples. The data could only be modeled empirically (see text) with two relaxation times.

sign of the Ni-O-Ni superexchange constant for low spin Ni^{3+} is unpredictable based on qualitative arguments. Therefore there is no a priori reason to expect J and J' to have the same sign. It is also possible that interlayer coupling of the N planes through the interaction J'' is possible, although this distance is twice that of the N - L layer distance. However, the number of N - N layer interactions, J'' , will be much larger than the number of N - L layer interactions, J' , due to the small number of nickel atoms in the L layers, δ . Figure 1 shows the structure of LiNiO_2 with J , J' , and J'' indicated. These ferromagnetic interactions (J' and J'') would explain the deviation from CW behavior of the susceptibility data below $T = 220$ K. Due to the in-plane frustration no long-range order occurs at this high temperature but short-range ferromagnetic correlations will form, as seen directly in recent SANS experiments (12). The irreversibilities may be due to spins in the L layers lining up with the field and causing nearby N layer spins to select an arrangement that best satisfies J' from the many configurations that are degenerate in zero field. It is conceivable that this could result

in a memory effect that persists up to temperatures above T_f . This can explain the much stronger *fc* magnetization observed in samples with larger concentrations of nickel atoms in the L layers, most notably sample E with 10% nickel in the L layers.

Interplanar interactions do *not* cancel by symmetry as some authors (6, 11) claim. Spins in the lithium layers lie directly over centers of basal plane triangles and therefore J' and/or J'' will add to the frustration since interplanar interactions prefer collinear spin arrangements and the in-plane frustration is best relieved by a noncollinear spin structure. Rastelli has shown that interplanar interactions of either sign will result in a distortion of the 120° spin arrangement (7).

It has long been believed that the necessary (but not sufficient) conditions for a spin glass are frustration and disorder (19). LiNiO_2 clearly satisfies both of these conditions. The effects of disorder on the RVB ground state are not well understood. However, one can imagine that small amounts of disorder will lift degeneracy of the $2^{3N/8}$ possible valence bond states. At low temperatures only a small subset of valence bond states are available and resonance will be inhibited. Without resonance the spins will appear frozen with random orientations as in a spin glass. Hence it is plausible that LiNiO_2 cannot support a spin liquid ground state because of the small amounts of disorder.

Some pyrochlore materials with ferromagnetic and antiferromagnetic interactions have also shown spin glass behavior at low temperatures. In pyrochlores the frustration is even more serious than in the case of LiNiO_2 . Two good examples are $\text{Y}_2\text{Mn}_2\text{O}_7$ (21) and $\text{Tb}_2\text{Mo}_2\text{O}_7$ (22), which both appear to be ferromagnets at high temperature and both have positive Weiss constants, θ . The low temperature susceptibility for $\text{Tb}_2\text{Mo}_2\text{O}_7$ shows a weak cusp at 25 K and irreversibilities very similar to LiNiO_2 below 25 K. $\text{Y}_2\text{Mn}_2\text{O}_7$ has a broad maximum at

7 K and irreversibilities in the susceptibility below this temperature. As with LiNiO_2 , these features are easily missed if the measurements are carried out at high fields. The heat capacity for $\text{Y}_2\text{Mn}_2\text{O}_7$ also shows complete entropy removal with no sharp features as observed in LiNiO_2 (11). However, unlike LiNiO_2 , short-range spin correlations are observable with neutrons for both $\text{Tb}_2\text{Mo}_2\text{O}_7$ and $\text{Y}_2\text{Mn}_2\text{O}_7$, most likely because of the larger moments ($S = 9/2$ for Tb^{3+} and $S = 3/2$ for Mn^{4+}). A third pyrochlore material $\text{Y}_2\text{Mo}_2\text{O}_7$ which shows classic spin glass behavior (23) (sharp cusp and history dependence) shows no signs of magnetic scattering (22) below T_f . The lack of scattering in this material could be due to the small Mo^{4+} moment ($S = 1$).

The lack of wide angle magnetic scattering in LiNiO_2 is not a unique situation as exemplified by $\text{Y}_2\text{Mo}_2\text{O}_7$ (22, 23). Recent calculations (24) show that interplanar interactions in rhombohedral lattice antiferromagnets (such as LiNiO_2) tend to move the magnetic scattering away from the expected $(\frac{1}{3}, \frac{1}{3}, l)$ Bragg angles. For ferromagnetic interplane interactions the scattering moves to lower Q and possibly right under the $(0, 0, 3)$ nuclear reflection. Disorder breaks up the ideal 120° spin structure and to a first approximation smears out the magnetic scattering in Q space. Moreover, even if the RVB ground state is preempted by partial spin freezing, local quantum fluctuations may severely weaken any short-range spin-spin correlations.

Future work on LiNiO_2 could proceed along a number of directions. Powder neutron diffraction with excellent statistics, on well characterized samples, may show some weak magnetic scattering. Single crystals of LiNiO_2 would be of interest because of the increased signal in the neutron scattering experiments. A systematic study of the Weiss constant θ as a function of x and δ would be of interest. On a more grand scale the search for spin liquid materials should

continue. Materials which do not support nonstoichiometric phases like $M'_xM_{2-x}O_2$ would be preferable.

Acknowledgments

We thank Mr. G. Hewitson for his assistance with the susceptibility measurements and Mr. Li Wu for his assistance with some of the figures. JNR would like to thank the Natural Sciences and Engineering Research Council of Canada (NSERC) for financial assistance in the form of a postdoctoral fellowship. We thank NSERC for funding a portion of this work under the strategic grant program.

References

1. P. W. ANDERSON, *Science* **235**, 1196 (1987); P. W. ANDERSON, G. BASKARAN, Z. ZOU, AND T. HSU, *Phys. Rev. Lett.* **58**, 2790 (1987); S. KIVELSON, D. ROKHSAR, AND J. SETHNA, *Phys. Rev. B* **35**, 8865 (1987).
2. P. W. ANDERSON, *Mater. Res. Bull.* **8**, 153 (1973); P. FAZEKAS AND P. W. ANDERSON *Philos. Mag.* **30**, 423 (1974).
3. D. A. HUSE AND V. ELSER, *Phys. Rev. Lett.* **60**, 2531 (1988); S. LIANG, B. DOUCOT, AND P. W. ANDERSON, *Phys. Rev. Lett.* **61**, 365 (1988); V. KALMEYER AND R. B. LAUGHLIN, *Phys. Rev. B* **39**, 11879 (1989).
4. V. ELSER, *Phys. Rev. Lett.* **62**, 2405 (1989); C. ZENG AND V. ELSER, *Phys. Rev. B* **42**, 8436 (1990).
5. A. B. HARRIS, A. J. BERLINSKY, AND C. BRUDER, *J. Appl. Phys.* **69**, 5200 (1991).
6. K. HIRAKAWA, H. KADOWAKI, AND K. UBUKOSHI, *J. Phys. Soc. Jpn.* **54**, 3526 (1985); K. HIRAKAWA AND H. KADOWAKI, *Physica B* **136**, 335 (1986).
7. E. RASTELLI AND A. TASSI, *J. Phys. C* **19**, L423 (1986).
8. J. B. GOODENOUGH, D. G. WICKHAM, AND W. J. CROFT, *J. Phys. Chem. Solids* **5**, 107 (1958); J. B. GOODENOUGH, D. G. WICKHAM, AND W. J. CROFT, *J. Appl. Phys.* **29**, 382 (1958).
9. V. W. BRONGER, H. BADE, AND W. KLEMM, *Z. Anorg. Allg. Chem.* **333**, 188 (1964).
10. J. P. KEMP, P. A. COX, AND J. W. HODBY, *J. Phys. Condens. Matter* **2**, 6699 (1990).
11. K. HIROTA, Y. NAKAZAWA, AND M. ISHIKAWA, *J. Mag. Mag. Mat.* **90/91**, 279 (1990); K. HIROTA, Y. NAKAZAWA, AND M. ISHIKAWA, *J. Phys. Condens. Matter* **3**, 4721 (1991).
12. H. YOSHIZAWA, H. MORI, K. HIROTA, AND M. ISHIKAWA, *J. Phys. Soc. Jpn.* **59**, 2631 (1990).

13. J. N. REIMERS, J. E. GREEDAN, AND M. SATO, *J. Solid State Chem.* **72**, 390 (1988).
14. R. J. HILL AND C. J. HOWARD, "Program for Rietveld Analysis of Fixed Wavelength X-ray and Neutron Powder Diffraction Patterns—Version LHPM 1," AAEC, Lucas Heights Research Laboratories, N.S.W., Australia.
15. U. VON SACKEN AND E. NODWELL, unpublished work.
16. J. R. DAHN, M. A. PY, AND R. R. HAERING, *Can. J. Phys.* **60**, 307 (1982).
17. R. ROTELLA, "IPNS Rietveld Analysis Package, Users Manual."
18. J. R. DAHN, U. VON SACKEN, AND C. A. MICHAL, *Solid State Ionics* **44**, 87 (1990).
19. K. BINDER AND A. P. YOUNG, *Rev. Mod. Phys.* **58**, 801 (1986).
20. S. MIYASHITA, *J. Phys. Soc. Jpn.* **53**, 44 (1984), and references therein.
21. J. N. REIMERS, J. E. GREEDAN, R. K. KREMER, E. GMELIN, AND M. A. SUBRAMANIAN, *Phys. Rev. B* **43**, 3387 (1991).
22. J. N. REIMERS, J. E. GREEDAN, S. L. PENNY, AND C. V. STAGER, *J. Appl. Phys.* **67**, 5967 (1990); J. E. GREEDAN, J. N. REIMERS, C. V. STAGER, AND S. L. PENNY, *Phys. Rev. B* **43**, 5682 (1991).
23. J. E. GREEDAN, M. SATO, X. YAN, AND F. S. RAZAVI, *Solid State Commun.* **59**, 895 (1986).
24. J. N. REIMERS, *Phys. Rev. B* **46**, 193 (1992).